Petroleum Science 19 (2022) 2175–2184

Contents lists available at ScienceDirect

Petroleum Science

journal homepage: www.keaipublishing.com/en/journals/petroleum-science

Original Paper

Study of the reinforced mechanism of fly ash on amphiphilic polymer gel

Bo-Bo Zhou [a, b], Wan-Li Kang [a, b, *], Hong-Bin Yang [a, b], Zhe Li [a, b], Li-Ping Ma [c], Shi-Tou Wang [c], Jia-Qi Wang [a, b], An-Qing Xie [a, b], Bauyrzhan Sarsenbekuly [d]

[a] Key Laboratory of Unconventional Oil & Gas Development (China University of Petroleum (East China)), Ministry of Education, Qingdao, 266580, Shandong, PR China
[b] School of Petroleum Engineering, China University of Petroleum (East China), Qingdao, 266580, Shandong, PR China
[c] Oil and Gas Technology Research Institute, Changqing Oilfield Branch Company, PetroChina, Xi'an, 710018, Shaanxi, PR China
[d] Kazakh-British Technical University, Almaty, 050000, Kazakhstan

ARTICLE INFO

Article history:
Received 15 November 2021
Received in revised form
26 May 2022
Accepted 29 May 2022
Available online 3 June 2022

Edited by Yan-Hua Sun

Keywords:
Reinforced amphiphilic polymer gel
Fly ash
Anti-aging stability
Conformance control

ABSTRACT

Amphiphilic polymer gels are widely used in heterogeneous reservoirs for conformance control technology. However, in high temperature and high salinity of calcium and magnesium reservoirs, amphiphilic polymer gels cannot maintain effective performance. In this work, a novel reinforced amphiphilic polymer gel (F-PADC gel) was prepared by physically mixing polymer solution and fly ash (FA), which is an extremely low cost material. The viscoelasticity and stability of the F-PADC gel were studied by rheometry and micro-rheometry. The reinforced mechanism of FA on amphiphilic polymer gels was revealed. The results show that the addition of FA can make the gel more robust with a denser network structure. On the fifth day, the elastic modulus (G') increases from 5.2 to 7.0 Pa and the viscosity modulus (G'') increases from 0.4 to 0.6 Pa at the frequency of 1 Hz, which improves the viscoelasticity of the gel system. More importantly, the F-PADC gel does not degrade after aging at 85 °C for 180 d. And its viscoelasticity increases obviously, G' and G'' increase to 110.0 Pa and 3.5 Pa, respectively, showing excellent anti-aging stability. Moreover, FA amphiphilic polymer gels have a good injectivity and a perfect plugging rate of 98.86%, which is better than that of sole amphiphilic polymer gels. This novel mixed FA amphiphilic polymer gels can prove to be a better alternative to conventional polymer gels to enhance oil recovery in high temperature and high salinity reservoirs.

1. Introduction

With the continuous development process of oil production, many oilfields have entered into high water-cut period (Bai et al., 2015a, 2015b; Li et al., 2020b), which leads to an ineffective circulation of injected water and a low production rate (Alhuraishawy et al., 2018; Liu et al., 2017). At present, the traditional plugging agents include polymer gels (Bai et al., 2022; Zhang et al., 2020b; Zhu et al., 2017a), microspheres (Yu et al., 2015), foam (Zhou et al., 2013) and preformed particle gels (PPGs) (Zhou et al., 2021b). Among them, polymer gels (Afolabi et al., 2019; Al-Shajalee et al., 2020; Kang et al., 2021) are the most widely used agents in oilfields due to the advantages of adjustable strength and low cost (Pu et al., 2019; Wang et al., 2020; Wu et al., 2022). In particular, polymer gel systems (Du et al., 2019; Liu and Seright, 2001; Sun et al., 2020; Young et al., 1989) can decrease the reservoir heterogeneity, so as to improve the sweep efficiency of reservoirs by water flooding (Crespo et al., 2014; Li et al., 2020a; Wang et al., 2017) and enhanced oil recovery (Saikia et al., 2020; Zhang et al., 2022; Zhu et al., 2021). In recent decades, significant work and research have been performed in this field.

Amphiphilic polymers (Zhang et al., 2019; Zhu et al., 2017b) refer to water-soluble polymers with a small number of hydrophobic groups in the hydrophilic main chain of the macromolecule. Due to the hydrophobic association between hydrophobic groups (Zhou et al., 2021a), the polymer has excellent temperature and salt resistance ability (Guo et al., 2021; Jia et al., 2011), which widens its

* Corresponding author. Key Laboratory of Unconventional Oil & Gas Development (China University of Petroleum (East China)), Ministry of Education, Qingdao, 266580, Shandong, PR China.
E-mail address: kangwanli@upc.edu.cn (W.-L. Kang).

https://doi.org/10.1016/j.petsci.2022.05.019

application range in oilfields (Yang et al., 2020). In addition to being an oil displacement agent, it is also used as the main component for preparing gel plugging agents (Yang et al., 2019a). Anti-aging stability is an important property for gel plugging agents, which determines the effective time of plugging. However, its anti-aging stability still needs to be further improved for an application in high temperature and salinity reservoirs. Some studies (Lashari et al., 2018, 2019) have shown that nanoparticles (Bai et al., 2018; Jia et al., 2020) can reinforce the anti-aging stability of amphiphilic polymer gels. For example, Yang et al. (2019b) constructed a nanoparticle-reinforced organic chromium gel using modified silica nanoparticles and amphiphilic polymers. They demonstrated that silica nanoparticle surface adsorbs free polymer molecules in solution, and forms molecular brushes due to charge attraction and hydrogen bonding. Thus, the stability of gels is improved. At 85 °C, the more silica nanoparticles are added, the more stable is the composite gel. When the concentration of silica nanoparticles is 1000 mg/L, the water-loss rate of the composite gel is 11% after 20 d.

Fly ash (FA) is a solid residual by-product of coal combustion in thermal power plants (Ma et al., 2013; Wojciech et al., 2015). FA usually presents a kind of gray superfine microspheres with uniform particle size and is composed of a large number of silica, alumina and other inorganic nanoparticles (Ahmad Zawawi et al., 2020; Wang, 2008). The colossal use of coal to meet the growing energy demand has led to an exponential growth of FA (Yao et al., 2015). Contrarily, FA utilisation is used only 1/4th of the total output (Wang, 2008). Unused FA is left exposed, causing environmental pollution and ecological imbalance (Nikolić et al., 2013). Maximizing the use of low-cost and easily available FA is the best option to deter ecological concerns and create economic opportunities (Hosseini et al., 2018).

The application of FA in oilfields is gradually emerging (Adewunmi et al., 2019; Ahdaya and Imqam, 2019; Liu et al., 2019). For example, FA can be used as fillers in polymers in order to improve their rheological properties (Liu et al., 2020). FA can be functionalized to replace API-grade drilling bentonite for drilling (Gautam et al., 2018; Ledesma et al., 2020). In order to enhance the viscoelastic characteristics of a gel, Adewunmi et al. (2017) incorporated coal fly ash in PAM/PEI gels. The results showed that the viscoelasticity of the gel could be increased by a maximum of 6 times. So it could be applied to water shutoff treatment in oil and gas wells (Adewunmi et al., 2019). Fakher et al. (2020) reinforced hydrolyzed polyacrylamide (HPAM) polymer solutions with the FA and studied the injectivity of this new reinforced polymer. The results showed that the most stable formulation was 0.5 and 1 wt% HPAM mixed with 0.5 and 1 wt% FA. As long as the FA was stable and evenly distributed along the HPAM network, there would be no pressure problem. Singh et al. (2018) improved the performance of nanocomposite gel systems by modifying FA to participate in the polymerization reaction. The nanocomposite gel system had sufficient gel strength (0.045 MPa) and a good plugging capacity at reservoir conditions (95.14%), but the preparation process was complicated. Few studies have been done on the direct blending of FA and amphiphilic polymer gels to improve the anti-aging stability in high temperature and salinity reservoirs. However, the mechanism of added FA on amphiphilic polymer gels remains unclear.

In this work, FA reinforced amphiphilic polymer gels were prepared by a physical mixing method. Viscoelasticity and stability of amphiphilic polymer gels (PADC gel) and FA reinforced amphiphilic polymer gels (F-PADC gels) were studied by rheometry and micro-rheometry, respectively. An anti-aging stability mechanism of FA reinforced amphiphilic polymer gels was proposed. The plugging performance was demonstrated by artificial sand pack plugging tests. The F-PADC gels represent a promising material for improving the heterogeneity of high temperature and high salinity reservoirs. Moreover, it is of great help for the recycling of fly ash and to improve environmental protection.

2. Experimental

2.1. Materials

All reagents and chemicals are chemically pure, purchased from Sinopharm Chemical Reagent Co., Ltd (Beijing, China) except as noted. The amphiphilic polymer was self-made in the laboratory and was named PADC, the preparation methods of which were described elsewhere (Zhu et al., 2017b). The organic chromium crosslinker agent is of industrial grade and obtained from Sinopec Shengli Oilfield (Dongying, China). The molecular structure of both is shown in Fig. 1. Fly ash is of experimental grade, purchased from Huifeng New Materials Co., Ltd. (Zhengzhou, China).

As can be seen from Fig. 2, FA is spherical with different particle sizes, and the average particle size is 2.8 μm. Silica accounted for the largest proportion of FA, followed by alumina, and a small part of other oxides. The zeta potential of FA and PADC was −24.34 and 4.7 mV, respectively, whereas that of FA/PADC suspension was −4.83 mV, all measured by the Zetasizer Nano (Malvern, UK) measurement. These test methods are shown in Supplementary Material.

2.2. Methods

2.2.1. Preparation of gel samples

The composition of simulated formation water is list in Table 1. The formulation of F-PADC gels was: 4000 mg/L PADC, 2500 mg/L organic chromium crosslinking agent and 1000 mg/L FA. The detailed preparation method was as follows. Firstly, 10,000 mg/L PADC mother liquor and 10,000 mg/L organic chromium mother liquor were prepared with formation water. 10 mL PADC mother liquor, 6.25 mL organic chromium mother liquor and 8.75 mL formation water were mixed with each other. Then 0.025 g of FA was added, stirred and dispersed evenly to obtain the gel solution. In order to eliminate the influence of air on the gelling performance, the solution was poured into a bottle, and then the cap was quickly sealed after N_2 was introduced for 5 min. Finally, the gelling condition was observed at 85 °C, and the gelling time and strength were determined. The PADC gels are formed without adding fly-ash.

2.2.2. Determination of gelation properties

The gelation time is an important property for gel systems. The bottle testing method is used to determine the gelation time because it is convenient and inexpensive. The gelation time is defined as the time at which the gel reaches the maximum strength with a code ranging from A to J (Sydansk, 2004), as shown in Table 2. 25 mL gel solution was added into the ampoule tube, which was placed in a pre-heated oven at 85 °C. The ampoule tubes were observed visually by taking them out from the oven and inverting it. The time of the maximum gel code was noted as the gelation time.

The strength of gel samples was measured by the breakthrough vacuum method. These experiments were conducted according to the procedure previously reported (Bai et al., 2015a). The dehydration volume of the gel was divided by the initial volume to determine the percentage of dehydration. The water-loss rate (R_{wl}) was calculated using the following equation:

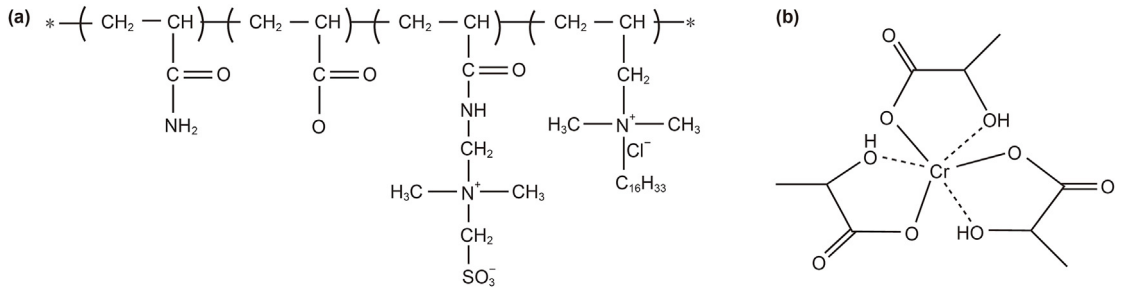

Fig. 1. The molecular structures of (**a**) PADC amphiphilic polymer and (**b**) organic chromium crosslinker.

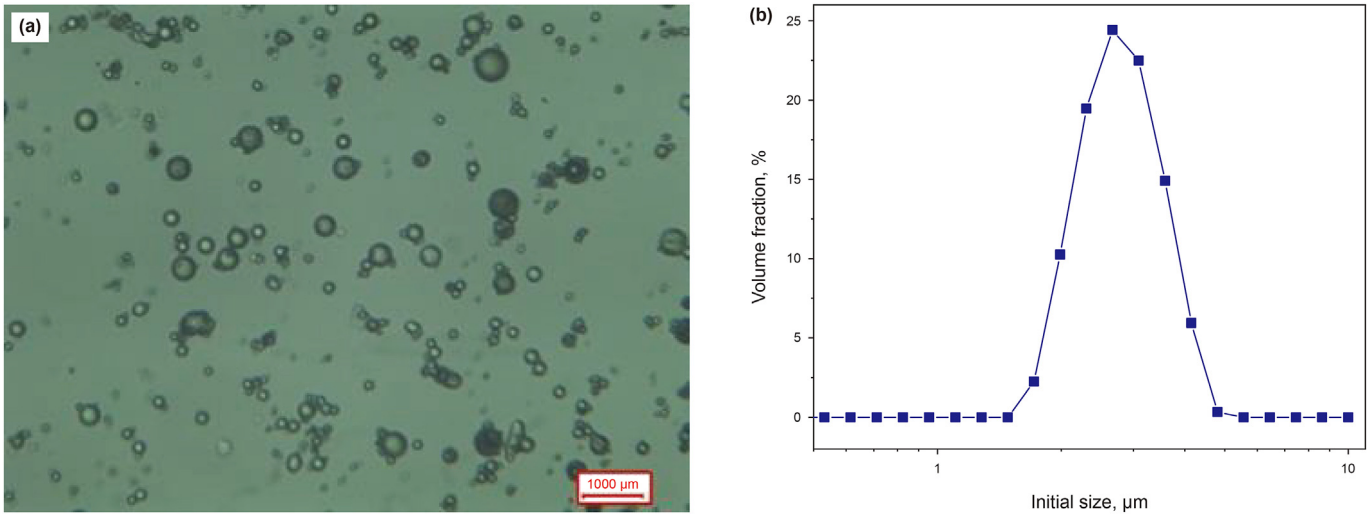

Fig. 2. (**a**) Micrographs and (**b**) particle size distribution of fly-ash.

Table 1
Compositions of simulated formation water.

Composition	Na^+	Ca^{2+}	Mg^{2+}	Cl^-	HCO_3^-	Total
Concentration, mg/L	27122.14	1505.71	1761.22	49594.84	129.27	80113.18

Table 2
Gel description corresponding to gel strength rating code (Sydansk, 2004).

Code	Gel description
A	No detectable gel formed
B	Highly flowing gel
C	Flowing gel
D	Moderately flowing gel
E	Barely flowing gel
F	Highly deformable non flowing gel
G	Moderately deformable non flowing gel
H	Slightly deformable non flowing gel
I	Rigid gel
J	Ringing rigid gel

$$R_{wl} = \frac{V_w}{V} \times 100\% \quad (1)$$

where V is the initial gel volume, cm^3; V_{water} is the dehydrated volume of the gel, cm^3.

The anti-aging stability of gel was evaluated under reservoir conditions by sealing the ampoule tubes and putting them in an oven at 85 °C for 180 d. The dehydration of the gel was checked regularly by reversing and observing the ampoule tubes.

2.2.3. Microscopic characterization

Atomic force microscopy (AFM, Bruker, USA) was used to observe the gel microstructure. The prepared polymer gel (about 10 μL) was placed on a clean mica plate by dropping. The sample was then placed in a vacuum spin coater and waited for a few minutes until the mica surface was dry. The AFM was used in the tap mode with a scanning angle of 0° and a scanning frequency of 1.50 Hz at 25 °C (Kang et al., 2019).

2.2.4. Rheology measurements

2.2.4.1. Rheology of gels. A MCR301 Rheometer (Anton Paar, Austria) with a plate system was used to measure the viscoelasticity of the gels. Firstly, a scanning stress was performed to determine the linear viscoelastic region. Then, the dynamic modulus of the gels at different frequencies (0.1–10 Hz) were measured in this linear viscoelastic region.

2.2.4.2. Micro-rheology of gels. According to the principle of Multi-speckle Diffusing Wave Spectroscopy (MS-DWS), the optical micro-rheometer (Formulation, France) was used for measuring the

micro-rheology of the gels (Zhang et al., 2020a). Its advantage is to test the gelation time and gel strength of polymer solutions without disturbances. The schematic diagram of measurements is shown in Fig. 3(a). The instrument consists of a laser source and a back-scattered light detector. During the experiment (Lashari et al., 2019), tracer particles were added to the PADC polymer solution. These tracer particles are continuously moving by Brownian motion, resulting in the deformation of scattering points. The detector detects the change of speckles, calculates the velocity of tracer particles, and finally obtains information on the mean square displacement (MSD) curve of tracer particles in the solution.

Then, Fig. 3(b) shows the graphical explanation of a typical MSD curve. The height of the plateau phase of the MSD curve represents the elasticity index (EI). The lower the plateau phase, the higher the EI. The slope of the last part of the MSD curve corresponds to the macroscopic viscosity index (MVI). The smaller the slope, the higher the MVI. The EI curves and the MVI curves of the PADC polymer solutions can be subsequently obtained by using a software to calculate the MSD curve (Lashari et al., 2019).

2.2.5. Plugging performance of gels

The plugging performance of a gel is evaluated in artificial sand packs, and its key parameters are shown in Table 3. The injection rate was 0.5 mL/min, and the experimental temperature was kept at 85 °C. The schematic diagram is shown in Fig. 4. Firstly, the simulated formation water was injected for 2.0 pore volume (PV) until the injection pressure was stabilized. Secondly, 2.0 PV of a polymer gel solution was injected. Thirdly, the artificial sand pack was placed into an oven at 85 °C for 5 d, so that the polymer may crosslink to form gel. Finally, the formation water was continuously injected until the injection pressure remained constant (Zhou et al., 2021a). The permeability and the plugging rate were calculated by the following equations:

$$k = \frac{Q\mu L}{A\Delta P} \tag{2}$$

$$\eta = \frac{k_0 - k'}{k_0} \times 100\% \tag{3}$$

where μ, A, Q and ΔP represent the fluid viscosity, the cross sectional area of the artificial sand pack, the injection rate and pressure difference, respectively; k_0 and k' are the initial and final permeability of the artificial sand pack, respectively.

3. Results and discussion

3.1. Gelling performance of F-PADC gels

The gelling performance of the gels is determined by the bottle testing method and the micro-rheometry. Gelation time and gel strength are important parameters to characterize gel properties. The gelation time determines the depth and extent of applied reservoirs. In addition, the gel should be strong enough to withstand the water flow.

The gel strength and breakthrough pressure of PADC gels are shown in Fig. 5(a) and (b). With the increase in time, the gel strength and the breakthrough pressure increase. The gel strength of PADC gels corresponds to code F after 4 d. The gelation time of the F-PADC gel is 3 d and the gel strength refers to code G. Furthermore, as shown in Fig. 6(a) and (b), the EI and MVI curves of PADC gels show an initial sharp increase and a rapid levelling off. With the increase in time, PADC quickly forms a dense spatial network structure with organic chromium as the crosslinking points. The spatial network structure limits the movement of tracer particles, i.e. a higher viscoelasticity is formed. Therefore, the EI and MVI values of amphiphilic polymer gels increase rapidly in a short time.

The maximum breakthrough pressure of PADC gels and F-PADC gels are 0.056 and 0.065 MPa, respectively. The addition of FA can shorten the gelation time and reinforce the gel strength. Besides, the EI and MVI curves of the F-PADC gel attain quicker a plateau and exhibit higher values. This indicates that the addition of FA can both accelerate the formation of the spatial network structure and improve the viscoelasticity of PADC gels. This is because the negatively charged FA particles act as adsorption points, and the positively charged polymer chains are intertwined to form the network structure more quickly via electrostatic attraction. For the cross-linking reaction between the organic chromium crosslinker and PADC, FA is used as an additive to enhance the network structural strength, thereby improving the viscoelasticity of the F-PADC gel.

3.2. Rheological properties of F-PADC gels

The viscosity modulus (G'') and the elastic modulus (G') of PADC gels and F-PADC gels with different gelation times are analyzed. In Fig. 7(a), it can be found that G' is higher than G'', indicating the dominance of the elastic behavior in both gels.

Besides, the viscoelasticity of F-PADC gels is higher than that of PADC gels at the same time. When the gelation time is 5 d, the

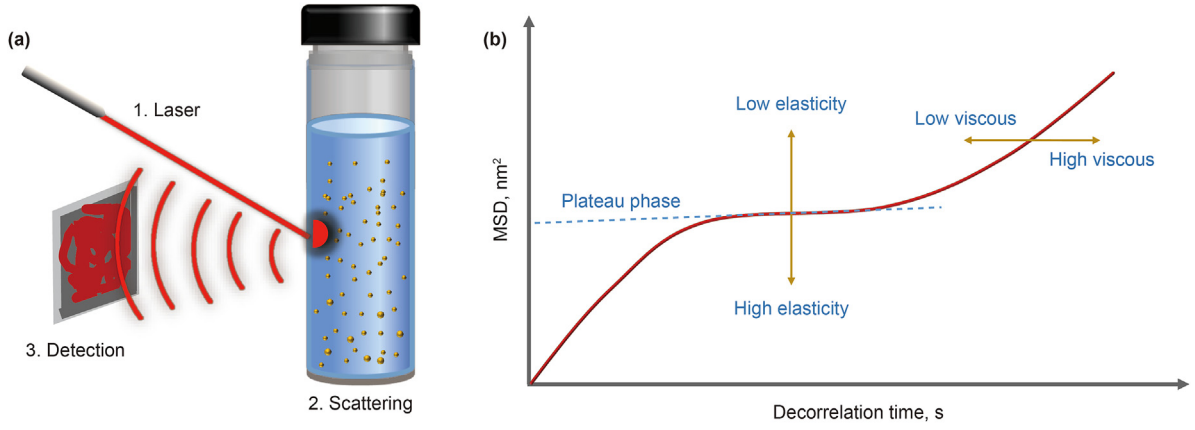

Fig. 3. (**a**) Measurement principle diagram of MS-DWS; (**b**) graphical illustration of MSD.

Table 3
Key parameters of artificial sand packs.

No.	Gel type	Length L, cm	Diameter d, cm	Porosity ϕ, %	Permeability k_0, μm^2
1	F-PADC gel	10.01	2.5	36.68	1.321
2	PADC gel	10.00	2.5	34.65	1.275

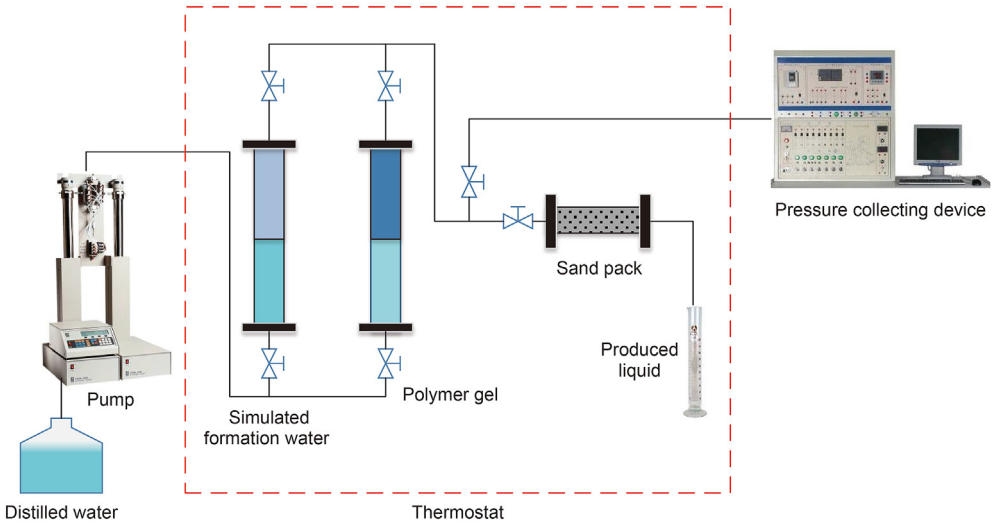

Fig. 4. Schematic of plugging experiments (Zhou et al., 2021a).

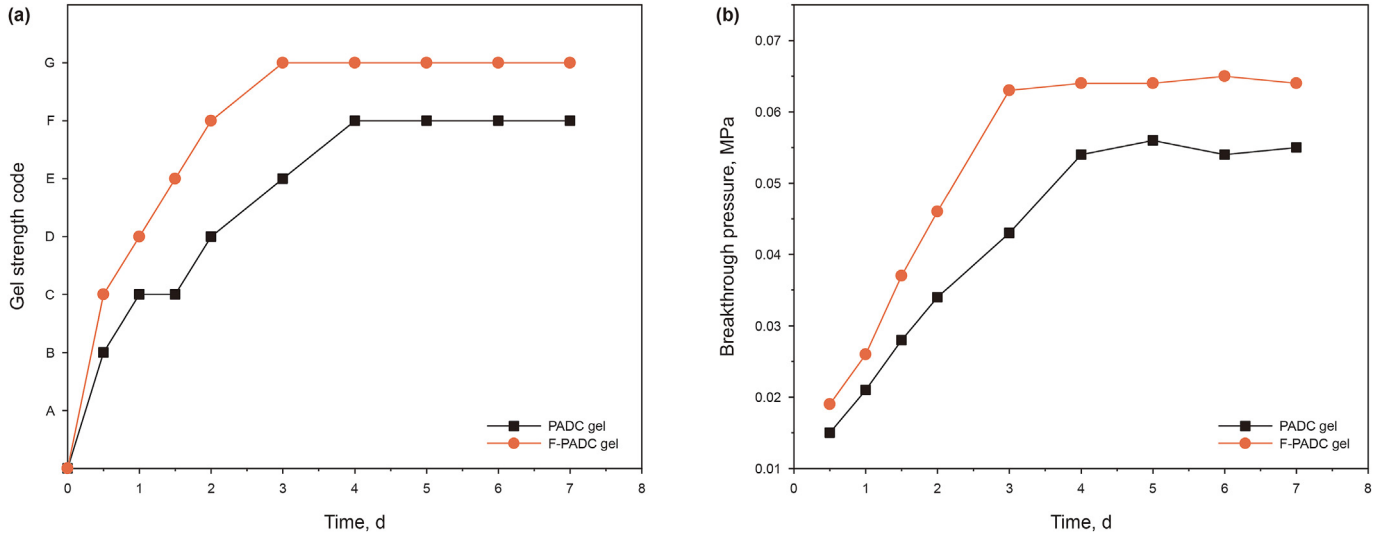

Fig. 5. (**a**) Gel strength code; (**b**) breakthrough pressure curves.

viscoelastic properties of F-PADC gels and PADC gels are greatly improved. This is because organic chromium crosslinks with the carboxyl group of the amphiphilic polymers as time increases, and the internal network structure density of the gels increases.

It is worth noting that the water loss rate of PADC gels is 33.5% at 60 d and completely loses its viscoelasticity after 180 d. When the gelation time reaches 180 d, F-PADC gels do not lose water, and the gel strength remains unchanged at the code G (as shown Fig. 8). The viscoelasticity of F-PADC gels is shown in Fig. 7(b). While G' increases from 7.0 to 110.0 Pa, the value of G'' increases from 0.6 to 3.5 Pa at the frequency of 1 Hz. This indicates that the addition of FA not only reinforces the anti-aging stability of amphiphilic polymer gels, but also increases its viscoelasticity.

3.3. Injection and plugging performance of F-PADC and PADC gels

Injection ability and plugging performance are also important parameters of polymer gels. They determine the conformance control effect of gels. Fig. 9 shows injection and plugging behavior of gels in artificial sand packs. As shown in Table 4, the plugging rates of PADC and F-PADC gels are 96.56% and 98.33%, respectively.

As seen from Fig. 9(a), the injection pressure of two artificial sand packs increases with the injection in polymer gel solutions. The injection pressure for the PADC gel solution rises to around

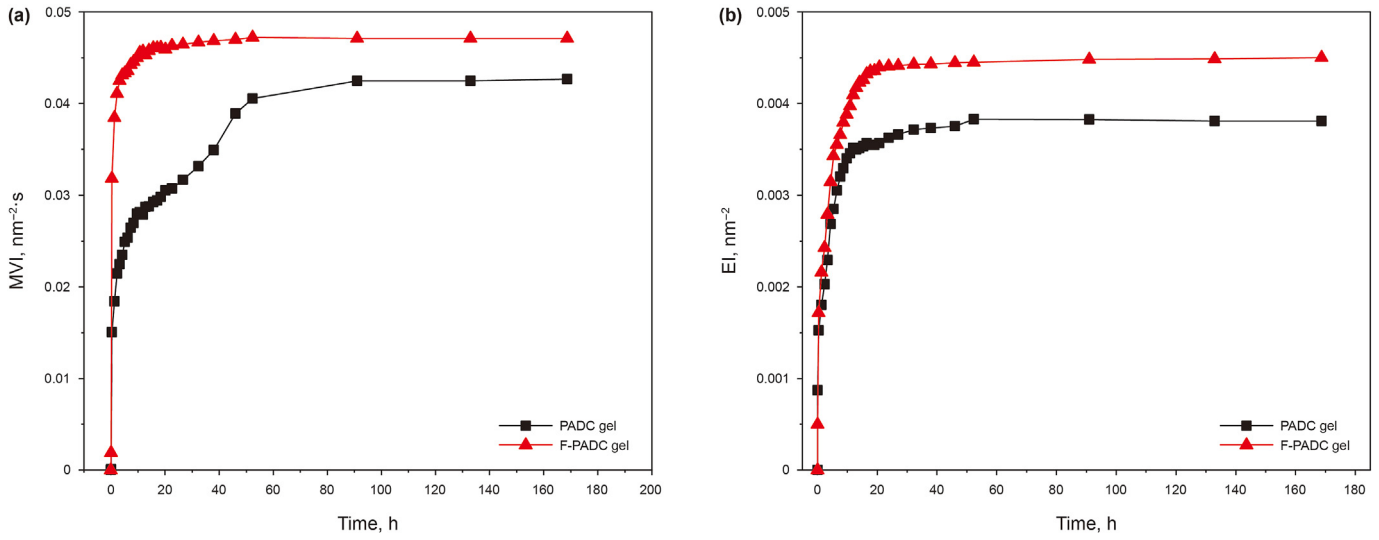

Fig. 6. (**a**) MVI curves of PADC and F-PADC gels; (**b**) EI curves of PADC and F-PADC gels ($T = 85$ °C).

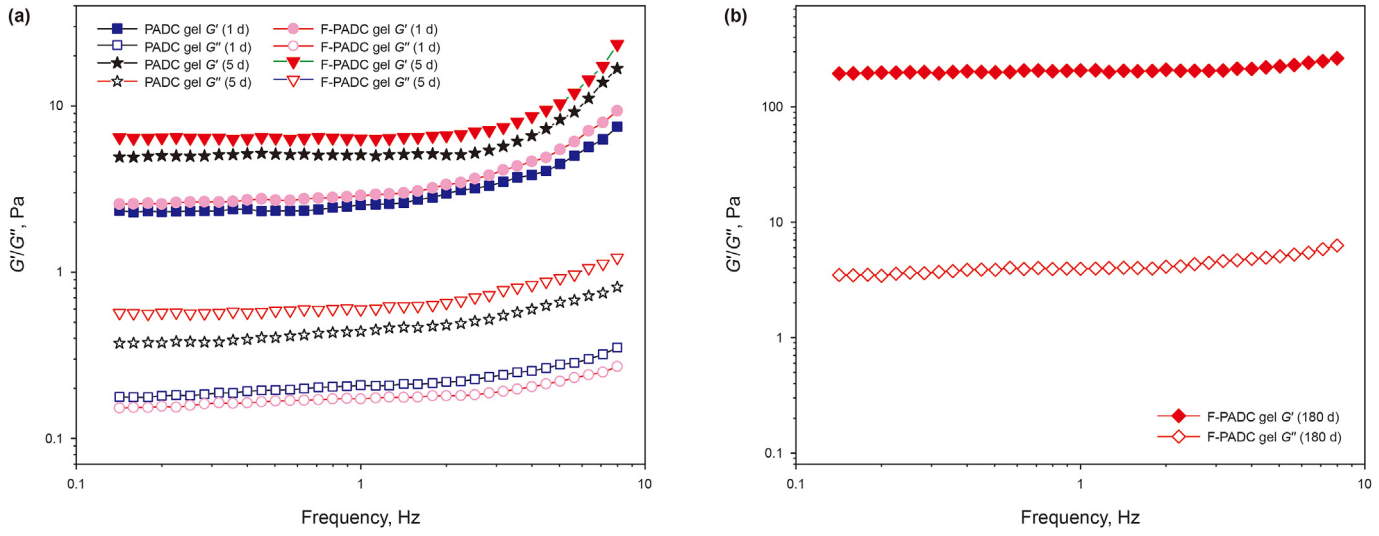

Fig. 7. Dynamic viscoelasticity curves of PADC and F-PADC gels after gelation. (**a**) 1, 5 d; (**b**) 180 d.

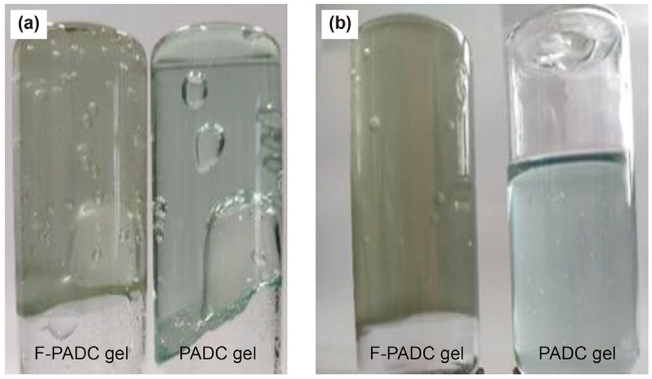

Fig. 8. Photographs of F-PADC and PADC gels after gelation. (**a**) 5 d; (**b**) 180 d.

6 kPa, and that for the F-PADC gel can rise to around 14 kPa. This indicates that the two polymer gel solutions have good injection ability. Due to the addition of FA, the F-PADC gel solution may block in the pore throat of the artificial sand pack, so the injection pressure is higher than for the PADC gel solution.

As shown in Fig. 9(b), the injection pressure increases with the formation water injection after gelation. When the pressure value reaches 42 kPa (breakthrough pressure), the pressure of the PADC gel deceases sharply and the gel appears at the outlet. This indicates that the formation water has formed channels in the artificial sand pack. Then, the pressure increases to a maximum value of 53 kPa, which is caused by the plugging during the movement of the gel block in the artificial sand pack. The breakthrough pressure of the F-PADC gel is 83 kPa, and the pressure continues to increase up to 87 kPa and then begins to decrease. This is because of its greater viscoelasticity and gel strength. Subsequently, the injection pressure of both gels eventually fluctuates and tends to become constant. The pressure fluctuation is due to the migration and the secondary blockage of some smaller gels in the artificial sand pack as the formation water is injected.

The final pressure of the artificial sand pack treated with the F-

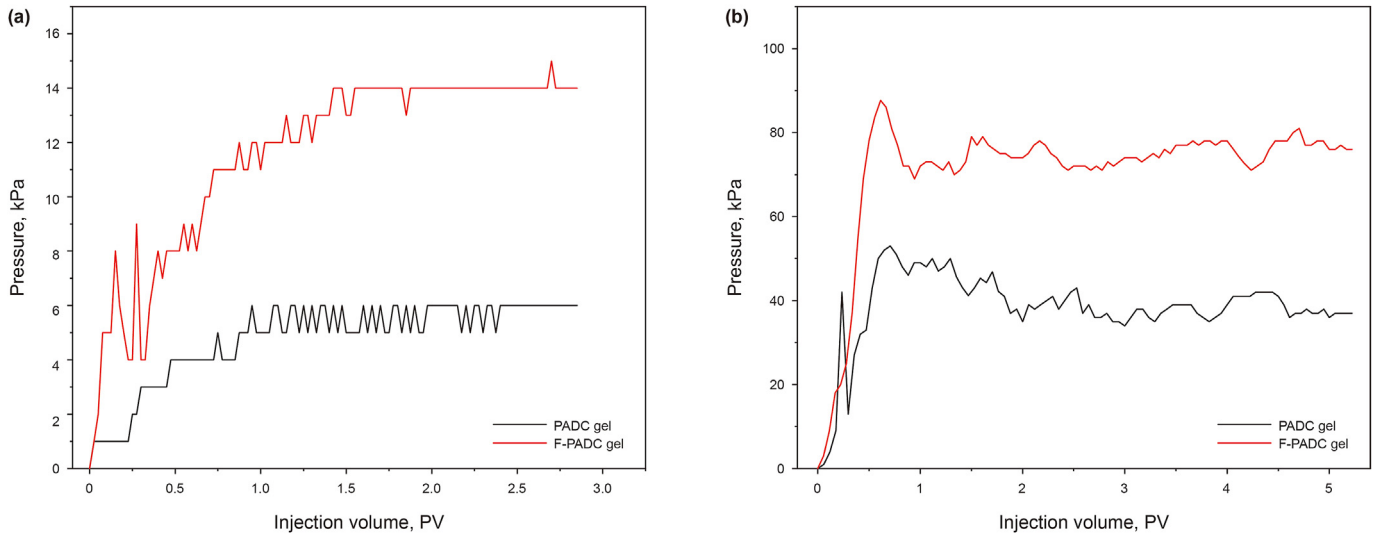

Fig. 9. (**a**) Injection pressure curves of PADC and F-PADC gels; (**b**) pressure curves of subsequent water.

Table 4
Experimental results of artificial sand packs.

No.	Gel type	Initial permeability k_0, μm^2	Final permeability k', μm^2	Plugging rate η, %	Breakthrough pressure, MPa
1	F-PADC gel	1.321	0.022	98.33	0.083
2	PADC gel	1.275	0.042	96.56	0.042

PADC gel maintains at around 77 kPa, and is 40 kPa higher as compared with that of the PADC gel after 5 PV water flooding. Therefore, this illustrates that the F-PADC gel has better plugging performance and flushing resistance than the PADC gel in high temperature and high salt reservoirs.

3.4. Reinforced mechanism of fly ash on the PADC gel

According to the above results, the F-PADC gel has higher viscoelasticity and stronger anti-aging stability. In order to analyze the role of FA in gel systems, AFM is used to study the network structure of PADC and F-PADC gels, respectively. The results are shown in Fig. 10 for a gelation time of 5 d. It can be observed that both the PADC gel (Fig. 10(a)) and the F-PADC gel (Fig. 10(b)) can form dense network aggregates. Moreover, the surface of the F-PADC gel structure is rougher due to the addition of FA. The highest peak of the F-PADC gel (1.8 μm) is much larger than that of the PADC gel (635.6 nm). This indicates that FA makes the gel forming a more robust network structure. The SEM results of the gel analysis are shown in Fig. S1 in Supplementary Material, which is consistent with the AFM results.

It concludes that FA could act as an inorganic additive to adhere onto the gaps of the gel skeleton, and reinforce the strength and stability of the gel structure. In addition, this evidence also explains why the F-PADC gel has better viscoelastic properties and stability from a micro-perspective point of view.

After adding the organic chromium crosslinker into the solution of the amphiphilic polymer, the chromium ion hydrate first hydrolyzes and polymerizes to form polynuclear hydroxyl bridged complex ions. At the same time, the amide group in the polymer molecules hydrolyzes to form the carboxyl group, and the cross-linking reaction occurs between the polynuclear hydroxyl bridged complex ion and the carboxyl group. The amphiphilic polymer molecules are further cross-linked by the chromium crosslinker, resulting in the formation of a complex and dense spatial network structure of amphiphilic polymer gels.

On the basis of amphiphilic polymer gels, inorganic FA can be used as reinforcing agent. The mechanism of reinforcing the gel can be described in Fig. 11 and concluded as follows: i) As a porous structure material, FA can be physically adsorbed onto the polymer molecules and chromium crosslinker through physical adsorption. It can be incorporated into the gel network structure and enhance the strength of the skeleton. ii) The special pore structure of FA can store water molecules lost in the polymer gel, so that the water molecules can be dynamically balanced between the gel structure and the pore structure, which can effectively reduce the dehydration of the composite gel. iii) Due to the negative charge on the surface of FA particles, the electrostatic attraction between FA and the positively charged amphiphilic polymer molecules can further enhance the strength of the cross-linked network structure.

Under the synergistic effect of the above three mechanisms, a more robust and denser network structure is formed inside the composite gel, and its viscoelastic properties also increase. Macroscopically, the F-PADC gel has a higher gel strength and breakthrough pressure, and can maintain a stable performance under adverse conditions such as high temperature aging.

4. Conclusions

Polymer gels of PADC and F-PADC with an organic chromium crosslinker are constructed. The addition of FA particles to an amphiphilic polymer gel solution can shorten the gelation time and improve the gel strength. The reinforced effect of FA on an amphiphilic polymer gel leads to a more robust and denser network structure. After 180 d of aging at high temperature, the strength of the F-PADC gel is constant and the viscoelasticity increases, indicating its excellent anti-aging stability. The reinforcement mechanism of added FA to F-PADC gels is summarized as follows. Firstly, FA can improve the skeleton strength of the gel by adsorption. Secondly, the special pore structure of FA particles can

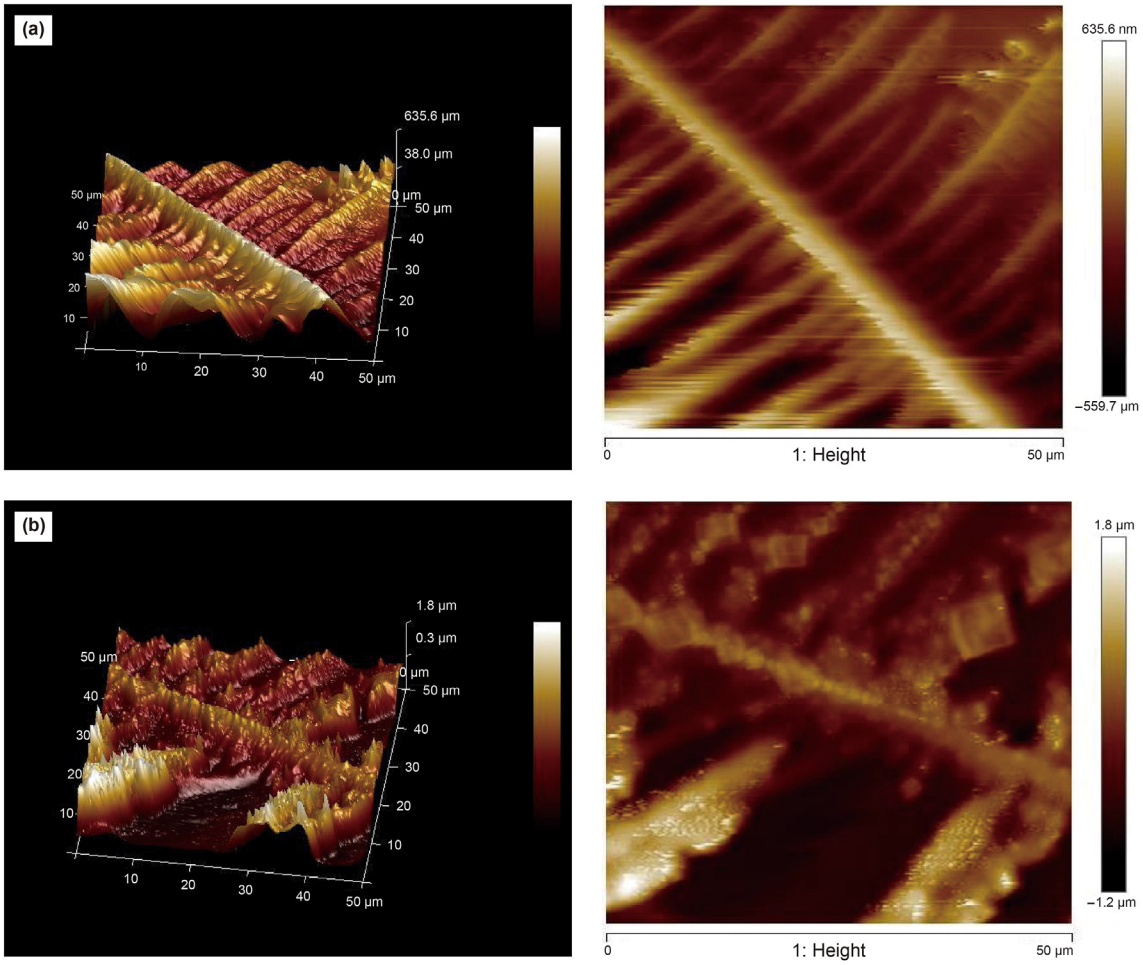

Fig. 10. AFM images of (**a**) PADC gel and (**b**) F-PADC gel.

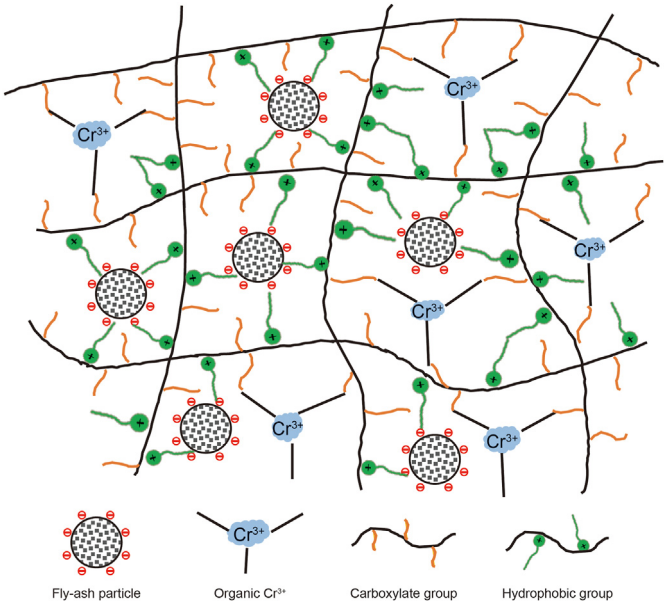

Fig. 11. Schematic diagram of the interaction network structure in F-PADC gels.

store water molecules lost in the polymer gel, thereby effectively reducing the dehydration of the gel. Thirdly, the negatively charged FA particle surface can attract the positively charged amphiphilic polymer molecules via electrostatic interaction, thereby reinforcing the stability and strength of the gel. Finally, the artificial sand pack results show that the F-PADC gel has a good injection performance and a higher plugging ability compared with PADC gels. This study shows that cheap and easily available FA can be used as an enhancer of amphiphilic polymer gels, so as to broaden the application scope of polymer gels in high temperature and high salinity reservoirs.

Acknowledgements

The work was supported by Key Program of National Natural Science Foundation of China (No. 52130401), National Natural Science Foundation of China (No. 52104055), China National Postdoctoral Program for Innovative Talents (No. BX20200386) and China Postdoctoral Science Foundation (No. 2021M703586).

Appendix A. Supplementary data

Supplementary data to this article can be found online at https://doi.org/10.1016/j.petsci.2022.05.019.

References

Adewunmi, A.A., Ismail, S., Owolabi, T.O., et al., 2017. Modeling the thermal behavior of coal fly ash based polymer gel system for water reduction in oil and gas wells.

J. Petrol. Sci. Eng. 157, 430–440. https://doi.org/10.1016/j.petrol.2017.07.019.
Adewunmi, A.A., Ismail, S., Owolabi, T.O., et al., 2019. Hybrid intelligent modelling of the viscoelastic moduli of coal fly ash based polymer gel system for water shutoff treatment in oil and gas wells. Can. J. Chem. Eng. 97 (11), 2969–2978. https://doi.org/10.1002/cjce.23436.
Afolabi, R.O., Oluyemi, G.F., Officer, S., Ugwu, J.O., 2019. Hydrophobically associating polymers for enhanced oil recovery – Part A: a review on the effects of some key reservoir conditions. J. Petrol. Sci. Eng. 180, 681–698. https://doi.org/10.1016/j.petrol.2019.06.016.
Ahdaya, M., Imqam, A., 2019. Fly ash Class C based geopolymer for oil well cementing. J. Petrol. Sci. Eng. 179, 750–757. https://doi.org/10.1016/j.petrol.2019.04.106.
Ahmad Zawawi, M.N.A., Muthusamy, K., Abdul Majeed, A.P.P., Muazu Musa, R., Mokhtar Albshir Budiea, A., 2020. Mechanical properties of oil palm waste lightweight aggregate concrete with fly ash as fine aggregate replacement. J. Build. Eng. 27, 100924. https://doi.org/10.1016/j.jobe.2019.100924.
Al-Shajalee, F., Arif, M., Machale, J., et al., 2020. A multiscale investigation of cross-linked polymer gel injection in sandstone gas reservoirs: implications for water shutoff treatment. Energy Fuels 34 (11), 14046–14057. https://doi.org/10.1021/acs.energyfuels.0c02858.
Alhuraishawy, A.K., Sun, X., Bai, B., Wei, M., Imqam, A., 2018. Areal sweep efficiency improvement by integrating preformed particle gel and low salinity water flooding in fractured reservoirs. Fuel 221, 380–392. https://doi.org/10.1016/j.fuel.2018.02.122.
Bai, B., Leng, J., Wei, M., 2022. A comprehensive review of in-situ polymer gel simulation for conformance control. Petrol. Sci. 19 (1), 189–202. https://doi.org/10.1016/j.petsci.2021.09.041.
Bai, B., Zhou, J., Yin, M., 2015a. A comprehensive review of polyacrylamide polymer gels for conformance control. Petrol. Explor. Dev. 42 (4), 525–532. https://doi.org/10.1016/S1876-3804(15)30045-8.
Bai, Y., Shang, X., Wang, Z., Zhao, X., 2018. Experimental study of low molecular weight polymer/nanoparticle dispersed gel for water plugging in fractures. Colloids Surf. A Physicochem. Eng. Asp. 551, 95–107. https://doi.org/10.1016/j.colsurfa.2018.04.067.
Bai, Y., , et al.Wei, F., Xiong, C., 2015b. Effects of fracture and matrix on propagation behavior and water shut-off performance of a polymer gel. Energy Fuels 29 (9), 5534–5543. https://doi.org/10.1021/acs.energyfuels.5b01381.
Crespo, F., Reddy, B.R., Eoff, L., Lewis, C., Pascarella, N., 2014. Development of a polymer gel system for improved sweep efficiency and injection profile modification of IOR/EOR treatments. In: International Petroleum Technology Conference. https://doi.org/10.2523/iptc-17226-MS.
Du, D., Pu, W., Tan, X., Liu, R., 2019. Experimental study of secondary crosslinking core-shell hyperbranched associative polymer gel and its profile control performance in low-temperature fractured conglomerate reservoir. J. Petrol. Sci. Eng. 179, 912–920. https://doi.org/10.1016/j.petrol.2019.05.006.
Fakher, S., Ahdaya, M., Imqam, A., 2020. Hydrolyzed polyacrylamide – fly ash reinforced polymer for chemical enhanced oil recovery: Part 1 – injectivity experiments. Fuel 260, 116310. https://doi.org/10.1016/j.fuel.2019.116310.
Gautam, S., Guria, C., Rajak, D.K., Pathak, A.K., 2018. Functionalization of fly ash for the substitution of bentonite in drilling fluid. J. Petrol. Sci. Eng. 166, 63–72. https://doi.org/10.1016/j.petrol.2018.02.065.
Guo, J., Zhang, S., Yang, Y., et al., 2021. Temperature-resistant and salt-tolerant mixed surfactant system for EOR in the Tahe Oilfield. Petrol. Sci. 18 (2), 667–678. https://doi.org/10.1007/s12182-020-00527-w.
Hosseini, T., De Girolamo, A., Zhang, L., 2018. Energy evaluation and techno-economic analysis of low-rank coal (Victorian Brown Coal) utilization for the production of multi-products in a drying–pyrolysis process. Energy Fuels 32 (3), 3211–3224. https://doi.org/10.1021/acs.energyfuels.7b03840.
Jia, H., Niu, C., Yang, X., 2020. Improved understanding nanocomposite gel working mechanisms: from laboratory investigation to wellbore plugging application. J. Petrol. Sci. Eng. 191, 107214. https://doi.org/10.1016/j.petrol.2020.107214.
Jia, H., Pu, W., Zhao, J., Liao, R., 2011. Experimental investigation of the novel phenol–formaldehyde cross-linking HPAM gel system: based on the secondary cross-linking method of organic cross-linkers and its gelation performance study after flowing through porous media. Energy Fuels 25 (2), 727–736. https://doi.org/10.1021/ef101334y.
Kang, W., Kang, X., Lashari, Z.A., et al., 2021. Progress of polymer gels for conformance control in oilfield. Adv. Colloid Interface Sci. 289, 102363. https://doi.org/10.1016/j.cis.2021.102363.
Kang, W., Zhang, H., Lu, Y., Yang, H., Besembaevna, O.Z., 2019. Study on the enhanced viscosity mechanism of the cyclodextrin polymer and betaine-type amphiphilic polymer inclusion complex. J. Mol. Liq. 296, 111792. https://doi.org/10.1016/j.molliq.2019.111792.
Lashari, Z.A., Kang, W., Yang, H., Zhang, H., Sarsenbekuly, B., 2019. Macro-rheology and micro-rheological study of composite polymer gel at high salinity and acidic conditions for CO_2 shut off treatment in harsh reservoirs for improving oil recovery. In: SPE/PAPG Pakistan Section Annual Technical Symposium and Exhibition. https://doi.org/10.2118/201175-MS.
Lashari, Z.A., Yang, H., Zhu, Z., et al., 2018. Experimental research of high strength thermally stable organic composite polymer gel. J. Mol. Liq. 263, 118–124. https://doi.org/10.1016/j.molliq.2018.04.146.
Ledesma, R.B., Lopes, N.F., Bacca, K.G., et al., 2020. Zeolite and fly ash in the composition of oil well cement: Evaluation of degradation by CO_2 under geological storage condition. J. Petrol. Sci. Eng. 185, 106656. https://doi.org/10.1016/j.petrol.2019.106656.
Li, Z., Wu, H., Hu, Y., et al., 2020a. Ultra-low interfacial tension biobased and catanionic surfactants for low permeability reservoirs. J. Mol. Liq. 309, 113099. https://doi.org/10.1016/j.molliq.2020.113099.
Li, Z., Xu, D., Yuan, Y., Wu, H., Bai, B., 2020b. Advances of spontaneous emulsification and its important applications in enhanced oil recovery process. Adv. Colloid Interface Sci. 277, 102119. https://doi.org/10.1016/j.cis.2020.102119.
Liu, J., Seright, R.S., 2001. Rheology of gels used for conformance control in fractures. SPE J. 6 (2), 120–125. https://doi.org/10.2118/70810-pa.
Liu, X., Nair, S., Aughenbaugh, K., van Oort, E., 2019. Mud-to-cement conversion of non-aqueous drilling fluids using alkali-activated fly ash. J. Petrol. Sci. Eng. 182, 106242. https://doi.org/10.1016/j.petrol.2019.106242.
Liu, X., Nair, S.D., Aughenbaugh, K.L., Juenger, M.C.G., van Oort, E., 2020. Improving the rheological properties of alkali-activated geopolymers using non-aqueous fluids for well cementing and lost circulation control purposes. J. Petrol. Sci. Eng. 195, 107555. https://doi.org/10.1016/j.petrol.2020.107555.
Liu, Y., Dai, C., You, Q., et al., 2017. Experimental investigation on a novel organic-inorganic crosslinked polymer gel for water control in ultra-high temperature reservoirs. In: SPE/IATMI Asia Pacific Oil & Gas Conference and Exhibition. https://doi.org/10.2118/186225-MS.
Ma, Y., Hu, J., Ye, G., 2013. The pore structure and permeability of alkali activated fly ash. Fuel 104, 771–780. https://doi.org/10.1016/j.fuel.2012.05.034.
Nikolić, I., Đurović, D., Blečić, D., Zejak, R., Karanović, L., Mitsche, S., Radmilović, V.R., 2013. Geopolymerization of coal fly ash in the presence of electric arc furnace dust. Miner. Eng. 49, 24–32. https://doi.org/10.1016/j.mineng.2013.04.007.
Pu, J., Geng, J., Han, P., Bai, B., 2019. Preparation and salt-insensitive behavior study of swellable, Cr3+-embedded microgels for water management. J. Mol. Liq. 273, 551–558. https://doi.org/10.1016/j.molliq.2018.10.070.
Saikia, T., Sultan, A., Barri, A.A., et al., 2020. Development of pickering emulsified polymeric gel system for conformance control in high temperature reservoirs. J. Petrol. Sci. Eng. 184, 106596. https://doi.org/10.1016/j.petrol.2019.106596.
Singh, R., Mahto, V., Vuthaluru, H., 2018. Development of a novel fly ash-polyacrylamide nanocomposite gel system for improved recovery of oil from heterogeneous reservoir. J. Petrol. Sci. Eng. 165, 325–331. https://doi.org/10.1016/j.petrol.2018.02.038.
Sun, X., Bai, B., Alhuraishawy, A.K., Zhu, D., 2020. Understanding the plugging performance of HPAM-Cr (III) polymer gel for CO_2 conformance control. SPE J. 25 (5), 3109–3118. https://doi.org/10.2118/204229-PA.
Sydansk, R.D., Al-Dhafeeri, A.M., Xiong, Y., Seright, R.S., 2004. Polymer gels formulated with a combination of high-and low-molecular-weight polymers provide improved performance for water-shutoff treatments of fractured production wells. SPE Prod. Facil. 19 (4), 229–236. https://doi.org/10.2118/89402-PA.
Wang, C., Zhong, L., Liu, Y., et al., 2020. Characteristics of weak-gel flooding and its application in LD10-1 Oilfield. ACS Omega 5 (38), 24935–24945. https://doi.org/10.1021/acsomega.0c03762.
Wang, L., Long, Y., Ding, H., Geng, J., Bai, B., 2017. Mechanically robust re-crosslinkable polymeric hydrogels for water management of void space conduits containing reservoirs. Chem. Eng. J. 317 (Complete), 952–960. https://doi.org/10.1016/j.cej.2017.02.140.
Wang, S., 2008. Application of solid ash based catalysts in heterogeneous catalysis. Environ. Sci. Technol. 42 (19), 7055–7063. https://doi.org/10.1021/es801312m.
Wojciech, Franus, Małgorzata, M., et al., 2015. Coal fly ash as a resource for rare earth elements. Environmental Science & Pollution Research.
Wu, W., Hou, J., Qu, M., Yang, Y., Zhang, W., Wu, W., Wen, Y., Liang, T., Xiao, L., 2022. A novel polymer gel with high-temperature and high-salinity resistance for conformance control in carbonate reservoirs. Petrol. Sci. https://doi.org/10.1016/j.petsci.2022.05.003.
Yang, H., Iqbal, M.W., Lashari, Z.A., et al., 2019a. Experimental research on amphiphilic polymer/organic chromium gel for high salinity reservoirs. Colloids Surf. A Physicochem. Eng. Asp. 582, 123900. https://doi.org/10.1016/j.colsurfa.2019.123900.
Yang, H., Kang, W., Zhang, H., et al., 2019b. The new development of amphiphilic polymer profile control agent in high temperature and high salinity reservoirs. In: Abu Dhabi International Petroleum Exhibition & Conference. https://doi.org/10.2118/197813-MS.
Yang, H., Zhang, H., Zheng, W., et al., 2020. Effect of hydrophobic group content on the properties of betaine-type binary amphiphilic polymer. J. Mol. Liq. 113358. https://doi.org/10.1016/j.molliq.2020.113358.
Yao, Z.T., Ji, X.S., Sarker, P.K., et al., 2015. A comprehensive review on the applications of coal fly ash. Earth Sci. Rev. https://doi.org/10.1016/j.earscirev.2014.11.016.
Young, T.S., Hunt, J.A., Green, D.W., Willhite, G.P., 1989. Study of equilibrium properties of Cr(III)/polyacrylamide gels by swelling measurement and equilibrium dialysis. SPE Reservoir Eng. 4 (3), 348–356. https://doi.org/10.2118/14334-PA.
Yu, X., Pu, W., Chen, D., et al., 2015. Degradable cross-linked polymeric microsphere for enhanced oil recovery applications. RSC Adv. 5 (77), 62752–62762. https://doi.org/10.1039/c5ra05366h.
Zhang, H., Yang, H., Zhou, B., et al., 2020a. Effects of cyclodextrin polymer on the gelation of amphiphilic polymer in inclusion complex. J. Mol. Liq. 305, 112850. https://doi.org/10.1016/j.molliq.2020.112850.
Zhang, S., Guo, J., Gu, Y., et al., 2020b. Polyacrylamide gel formed by Cr(III) and phenolic resin for water control in high-temperature reservoirs. J. Petrol. Sci. Eng. 194, 107423. https://doi.org/10.1016/j.petrol.2020.107423.
Zhang, T., Ge, J., Wu, H., Guo, H., Jiao, B., Qian, Z., 2022. Effect of AMPS(2-acrylamido-2-methylpropane sulfonic acid) content on the properties of polymer gels.

Petrol. Sci. 19 (2), 697–706. https://doi.org/10.1016/j.petsci.2022.01.006.
Zhang, X., Yang, H., Wang, P., et al., 2019. Construction and thickening mechanism of amphiphilic polymer supramolecular system based on polyacid. J. Mol. Liq. 286, 110921. https://doi.org/10.1016/j.molliq.2019.110921.
Zhou, B., Kang, W., Yang, H., et al., 2021a. The shear stability mechanism of cyclodextrin polymer and amphiphilic polymer inclusion gels. J. Mol. Liq. 328, 115399. https://doi.org/10.1016/j.molliq.2021.115399.
Zhou, B., Kang, W., Yang, H., et al., 2021b. Preparation and properties of an acid-resistant preformed particle gel for conformance control. J. Petrol. Sci. Eng. 197, 107964. https://doi.org/10.1016/j.petrol.2020.107964.
Zhou, W., Dong, M., Wang, X., 2013. Polymer/gel enhanced foam flood for improving post-waterflood heavy oil recovery. SPE Heavy Oil Conference, doi:10.2118/165430-MS.
Zhu, D., Deng, Z., Chen, S., 2021. A review of nuclear magnetic resonance (NMR) technology applied in the characterization of polymer gels for petroleum reservoir conformance control. Petrol. Sci. 18 (6), 1760–1775. https://doi.org/10.1016/j.petsci.2021.09.008.
Zhu, D., Bai, B., Hou, J., 2017a. Polymer gel systems for water management in high-temperature petroleum reservoirs: a chemical review. Energy Fuels 31 (12), 13063–13087. https://doi.org/10.1021/acs.energyfuels.7b02897.
Zhu, Z., Kang, W., Yang, H., et al., 2017b. Study on salt thickening mechanism of the amphiphilic polymer with betaine zwitterionic group by β-cyclodextrin inclusion method. Colloid Polym. Sci. 295 (10), 1887–1895. https://doi.org/10.1007/s00396-017-4169-7.